Bactericidal effects of low-temperature atmospheric-pressure air plasma jets with no damage to plant nutrient solutions

Retsuo Kawakami[*,1], Mutsumi Aihara[1], Takuto Izumi[1], Akihiro Shirai[1], and Takashi Mukai[2]

[1] *Graduate School of Technology, Industrial and Social Sciences, Tokushima University, Tokushima 770-8506, Japan*

[2] *Nichia Corporation, Anan, Tokushima 774-0044, Japan*

* Corresponding author. E-mail: retsuo@ee.tokushima-u.ac.jp

Abstract

The bactericidal effects of air plasma jets produced with a twisted wire-cylindrical electrode configuration were clarified in terms of plasma-induced damage to plant nutrient solutions. The bacterial suspensions were directly irradiated with air plasma jets using a low gas flow rate, which was shown to significantly inactivate the bacteria suspended in the solutions without reducing the nutrient concentrations. However, the plasma irradiation time required for inactivation depended on the type of bacteria; *Escherichia coli* (*E. coli*) and *Bacillus subtilis* (*B. subtilis*) were inactivated in 20–30 s, while *Staphylococcus aureus* (*S. aureus*) required 7 min. The inactivation of *E. coli* and *B. subtilis* decreased with increasing air gas flow rate, whereas the inactivation of *S. aureus* was independent of the rate. The inactivation could be attributed to a greater number of reactive oxygen and nitrogen species (RONS) from the air plasma jet, including O_2 molecules in the feeding gas attaching to the bacterial suspension surface, which do not harm the nutrient components. This can be derived from the results; the air-plasma-jet-activated nutrient solutions (RONS introduced in the solutions) and the N_2 plasma jets had only a limited inactivation effect on the bacteria suspended in the solutions.

Keywords: direct irradiation with air plasma jet, twisted wire-cylindrical electrode configuration, bacterial inactivation in plant nutrient solution, no reduction of plant nutrient components, reactive oxygen and nitrogen species

1. Introduction

In recent years, food security has become an increasingly important issue because climate change and global warming have influenced the efficiency of agricultural production [1−5]. The artificial cultivation of plants (a plant factory) is a promising technology for improving food security [6−10]. Crops in plant factories can be successfully grown using circulating hydroponic systems, without the influence of environmental changes. Plant growth is accomplished by the absorption of nutrients from hydroponic nutrient solutions instead of from soil [11,12]. However, contamination of hydroponic nutrient solutions by pathogenic bacteria is a significant issue in plant factories because these circulating systems can rapidly spread pathogens throughout the factory [13,14]. Environment-conscious technologies for disinfecting hydroponic nutrient solutions are required for the development of future plant factories.

The use of ultraviolet light-emitting devices (UV-LEDs) is convenient and environmentally sound because it requires no harmful chemicals and produces no hazardous by-products [14]. UV irradiation systems based on LEDs have successfully inactivated *Escherichia coli* (*E. coli*) in hydroponic nutrient solutions [14]. However, there is a critical problem with the use of UV irradiation, since it reduces the concentration of iron in hydroponic nutrient solutions by forming iron-based precipitates, thereby inhibiting the growth of crops [15]. The reduction in iron content or the formation of iron-based precipitates is thought to be attributed predominantly to the UV-induced degradation of iron chelates contained in the iron content in nutrient solutions [16].

This study focuses on low-temperature atmospheric-pressure plasma technologies as an alternative approach for disinfecting hydroponic nutrient solutions. These plasmas have bactericidal activity due to reactive oxygen and nitrogen species (RONS) [17,18]. The exact mechanism of their inhibitory effect on microbial growth remains unclear, but three pathways have been proposed. These include direct permeabilization of the cell

membrane or wall leading to leakage of cellular components, critical damage to intracellular proteins, and damage to deoxyribonucleic acid (DNA) [18]. Low-temperature atmospheric-pressure plasmas are environmentally sound because they do not use harmful chemicals, as is the case with UV-LED. They are also convenient because they can easily be produced indoors and outdoors without using vacuum equipment. Therefore, various low-temperature atmospheric-pressure plasma technologies have recently gained attention in agricultural applications [19−24].

In an earlier study, Yasui *et al*. [25] inactivated the fungus, *Fusarium oxysporum*, suspended in plant nutrient solutions with submerged liquid plasmas. The plasmas were produced using a barrier-type surface discharge electrode configuration consisting of a powered sheet electrode in contact with the solution and an electrically grounded electrode. The powered sheet electrode had a hole with a diameter of 1 mm, through which various types of gases were fed into the solution to generate submerged liquid plasmas. The resultant plasma generated in O_2 gas inactivated the fungus in 5 min. In the case of submerged liquid plasmas generated in He and Ar gases, the fungus was sufficiently inactivated within 20 min; however, the plasma with the air gas showed a weak bactericidal effect. Furthermore, plasma-induced damage to plant nutrient solutions was not clarified in the aforementioned study [25]. Therefore, a more detailed understanding of the interactions between plant nutrient solutions and low-temperature atmospheric-pressure air plasmas is required to further enhance the bactericidal effect of nutrient solutions without causing plasma-induced damage to the nutrient solutions.

The purpose of the present study was to investigate the bactericidal effects of low-temperature atmospheric-pressure air plasma jets with various gas flow rates on plant nutrient solutions in terms of plasma-induced damage to those solutions. Specifically, we clarified whether air plasma jet irradiation inactivates bacteria suspended in plant nutrient solutions without reducing the concentration of nutrient components, such as iron. A

plasma jet device developed by Kawakami *et al*. [26] was used in this study. The air plasma jet was produced with a twisted wire-cylindrical electrode configuration (TWCEC) of the developed plasma jet device [26]. The device has the advantage that air plasma plumes of 3 mm in diameter produced by the TWCEC are in direct contact with irradiated objects. This diameter is larger than those produced by the hollow-electrode configuration (HEC) [27] and the rod-cylindrical electrode configuration (RCEC) [28,29]. The diameters of the HEC- and RCEC-produced plasma plumes were 1 mm. Therefore, TWCEC-produced plasma jet irradiation causes a strong interaction between the air plasma jet and the bacterial suspension, resulting in a high bactericidal effect. This method also utilizes ambient air as the feed gas, which promotes resource conservation. Some researchers have used Ar-based plasma jets with O_2 and H_2O_2 vapor [30,31], which does not conserve resources because of the high flow rate of the feed gas (> 1 L/min).

The bacteria suspended in the nutrient solution were *E. coli* American Type Culture Collection (ATCC) 25922 [32], *Bacillus subtilis* (*B. subtilis*) ATCC 6633 [33], and *Staphylococcus aureus* (*S. aureus*) ATCC 25923 [34]. These were chosen as model microorganisms in the present study because there are no globally uniform evaluation standards for quality control of plant nutrient solutions. *E. coli* is a disinfection indicator according to the evaluation standards for plant nutrient solutions for plant cultivation in Japan. The other two types of bacteria are also typical indicators of disinfection.

In addition to iron content, phosphorus, potassium, and nitrogen contents in plant nutrient solutions after plasma jet irradiation were measured using optical absorption spectroscopy [35] and the ion-selective electrode method [36]. Along with the bactericidal effects, changes in the nutrient solution content were investigated by changing the plasma irradiation time. The characteristics of air-plasma-jet-irradiated nutrient solutions were compared to with those of N_2-plasma-jet-irradiated nutrient solutions and air-plasma-jet-activated nutrient solutions (PASs). The present study allows for a clearer understanding

of the effects of air plasma jet irradiation on plant nutrient solutions, and provides relevant information for the practical application of air plasma jets in the disinfection of plant nutrient solutions without causing damage to these solutions.

2. Experimental procedure

Plant nutrient solutions were purchased from Kyowa Corp. Ltd. (Japan). They were prepared by mixing 100 mL of distilled water with 400 μL of plant nutrient solution while stirring. The bacteria suspended in the nutrient solutions were *E. coli* ATCC 25922 [32], *B. subtilis* ATCC 6633 [33], and *S. aureus* ATCC 25923 [34], as described above. These bacteria were cultured in Luria-Bertani (LB) broth at 37 °C for 18 h. The LB broth was composed of 97.5 wt% distilled water, 1.0 wt% tryptone [37], 1.0 wt% NaCl, and 0.5 wt% yeast extract. The cultured bacterial suspensions were centrifuged at $8 \times 10^3 \times g$ for 3 min to remove the LB broth and then washed three times with sterilized phosphate-buffered saline (PBS, pH 7.5), where g is the gravitational acceleration. Finally, a 30 mL sample solution with a concentration of 5×10^6 colony-forming units per milliliter (CFU/mL) was prepared by mixing a 29.7 mL nutrient solution at a concentration of 4×10^3 ppm with a 300 μL bacterial suspension. A 5 mL sample solution was placed in a sterilized dish (Coning #430588) and then irradiated with an air plasma jet. After the plasma jet irradiation, the irradiated sample solutions were serially diluted 10-fold with PBS. A 100 μL diluted sample solution was plated on an agar plate of LB broth and incubated at 37 °C for 18 h.

After incubation, the common logarithm (log) of the bacterial colonies grown on the agar plate was evaluated using the colony counting method [38,39]. The bacterial log number was measured three times for each sample solution, and the data were averaged. The results are displayed as average values, including standard deviations. Specifically, the log survival ratio was estimated from the equation $\log(N_t/N_0)$, where N_t is the colony

158 count of the irradiated sample and N_0 is the colony count of the sample before irradiation.
159 The obtained data were statistically analyzed using either the two-tailed or unpaired t-test
160 or the Tukey-Kramer test (Excel Tokei ver. 7.0, Esumi Corp. Ltd., Japan).
161 The bacteria suspended in the nutrient solutions were observed before and after plasma
162 irradiation using field-emission scanning electron microscopy (FE-SEM, S-4700, Hitachi
163 High-Technologies, Japan) to clarify the changes in the bacterial structures caused by air
164 plasma jet irradiation. The bacteria were collected using a filter membrane with pores of
165 0.2 μm in diameter. The collected bacteria were immobilized with a 2% glutaraldehyde
166 and 2% osmium tetroxide solution and observed at a magnification of 10^4 × using FE-
167 SEM.
168 The concentration of iron in the sample solution was determined using reduction-and-
169 bathophenanthroline absorptiometry (DPM2-Fe-D, Kyoritsu Chemical Check Lab. Corp.,
170 Japan) with a portable multiparameter water analyzer (DPM-MTSP, Kyoritsu Chemical-
171 Check Lab. Corp., Japan). The phosphorus content in the sample solution was assessed
172 using molybdenum blue absorptiometry (DPM2-PO4, Kyoritsu Chemical Check Lab.
173 Corp., Japan) with the same portable multiparameter water analyzer. The potassium
174 content of the sample solution was evaluated using a potassium ion meter based on the
175 ion-selective electrode method (LAQUAtwin K-11, Horiba, Japan). The concentration of
176 nitrogen in the sample solution was determined using a nitric acid ion meter based on the
177 ion-selective electrode method (LAQUAtwin NO3-11, Horiba, Japan).
178 The sample solution placed in the sterilized dish was irradiated with TWCEC-
179 produced air plasma jets at gas flow rates of 1 L/min, 3 L/min, and 5 L/min, as shown in
180 Fig. 1. The irradiation time of the air plasma jet varied in the range of 0–7 min. The sample
181 solution was positioned such that the distance from the jet nozzle to the surface of the
182 solution was 3 mm. The inner and outer diameters of the glass jet nozzle were 3 mm and
183 6 mm, respectively. The feeding gas used was ambient air at room temperature (22–25 ℃)

184 with a relative humidity of 40–55%. This gas was fed into the jet nozzle using an air
185 compressor. The copper cylindrical electrode in the TWCEC was electrically grounded,
186 and the tungsten twisted wires were powered using a 100 kHz bipolar impulse waveform
187 generator with a repetition frequency of 10 kHz (TE-HVP1010K300-NP, Tamaoki
188 Electronics Corp. Ltd., Japan). The root-mean-square (RMS) values of the applied
189 impulse voltage and the discharge current flowing into the sample solution were 2.7 kV
190 [26] and 100 mA, respectively. This current value showed little change when the gas flow
191 rate was increased.

192 The UV released from the air plasma jet was caused by the emission of the N_2 second
193 positive system, 2P(v', v), where v' and v are the vibrational quantum numbers of the
194 upper and lower states, respectively [26]. The intensity of the 337 nm UV associated with
195 2P(0,0) was the highest in the N_2 second positive system at 170 μW/cm^2, as measured
196 with an optical power meter (Nova II, Ophir Optonics Solutions Ltd., Japan), which was
197 an order of magnitude less than that emitted from the Ar plasma jet [26]. Details of the
198 air plasma jet device can be found in the literature [26].

199

200 **3. Results**

201 Figure 2(a) shows the dependence of the log survival ratio of *E. coli* suspended in the
202 nutrient solution irradiated with the air plasma jet at a gas flow rate of 1 L/min on
203 irradiation time. A small log survival ratio indicates a high inactivation of *E. coli*. The log
204 survival ratio significantly reduced from 0 to approximately −5.5 as the irradiation time
205 increased from 0 to 30 s. This result suggests that 30 s irradiation of the air plasma jet at
206 1 L/min inactivated the viable cell number of *E. coli* by approximately five orders of
207 magnitude. In contrast, the log survival ratio increased from −5.5 to −3.5 when the air gas
208 flow rate increased from 1 to 5 L/min, as shown in Fig. 2(b). This result suggests that an
209 increase in airflow rate lowered the inactivation of *E. coli*. The lowered inactivation can

be related to a suppression of increased electrode or gas temperature induced by an increase in the air gas flow rate [40]. Temperature suppression can decrease the density and temperature of the air plasma jet attaching onto the sample solution, thereby decreasing the number of RONS required for inactivation. Thus, an increase in the air gas flow rate contributed to the lowered inactivation.

A similar result was observed for the inactivation of *B. subtilis*, as shown in Fig. 3. The log survival ratio significantly decreased from 0 to −4 as the irradiation time lengthened from 0 to 20 s and then increased as the gas flow rate increased, as was the case with *E. coli*. This result suggests that the viable cell number of *B. subtilis* was inactivated by five orders of magnitude with 20 s of irradiation of the air plasma jet at 1 L/min. Consequently, the inactivation of *B. subtilis* was evaluated to be 5×10^3 CFU/mL/s, which was similar to that of *E. coli*.

As shown in Fig. 4(a), a different result was observed for the inactivation of *S. aureus* in relation to staphyloxanthin, which suppresses oxidative stress [41,42]. The irradiation time required to significantly inactivate *S. aureus* was longer than those of *E. coli* and *B. subtilis*. Specifically, the log survival ratio of *S. aureus* was reduced to −5 with 7 min irradiation of air plasma jet at 1 L/min. As shown in Fig. 4(b), the log survival ratio of *S. aureus* did not change when the air gas flow rate was increased from 1 to 5 L/min, as opposed to the results with the other types of bacteria used. This suggest that the inactivation of *S. aureus* is independent of the air gas flow rate because the number of RONS generated in the air plasma jet would be sufficiently large to inactivate *S. aureus* even at high gas flow rates because of the long irradiation time (7 min).

Figure 5 shows a comparison between the SEM images of the bacteria before and after air plasma jet irradiation. The damage scars or damage marks caused by the air plasma jet depended on the type of bacteria. Cell cleavage was observed for *E. coli* and *B. subtilis*, but not for *S. aureus*. The differences observed in the SEM results agreed with

236 those reported in the literature [43]. The inactivation of *E. coli* and *B. subtilis* could be
237 attributed to the damage to the cell wall structures by the air plasma jet, whereas that of
238 *S. aureus* could be caused by intracellular or DNA damage from the air plasma jet [43].
239 Figure 6 shows the variations in nutrient composition concentrations in the nutrient
240 solutions irradiated with the air plasma jet at 1 L/min in relation to irradiation time. The
241 maximum irradiation time was set to the time required for significant inactivation of *S.*
242 *aureus* (7 min). The Fe content concentration remained the same as before irradiation
243 with an irradiation time of 7 min, even though the air plasma jet emitted UV due to the
244 N_2 second positive system [26]. This result differs from that induced by UV-LED
245 irradiation, which reduced the Fe content concentration [15]. The K and P concentrations
246 also remained the same as those before irradiation as the irradiation time increased.
247 However, the N concentration increased with increasing irradiation time, indicating a
248 positive effect on the nutrient solution because N is essential for plant growth [44]. Thus,
249 air plasma jet irradiation was found to cause no damage to the nutrient solution, as
250 opposed to the results with UV-LED irradiation.
251 Figure 7 shows a comparison between the log survival ratios of *E. coli*, *B. subtilis*,
252 and *S. aureus* suspended in distilled water and plant nutrient solutions irradiated with the
253 air plasma jet at 1 L/min for 30 s, 20 s, and 7 min, respectively. In the case of *E. coli*, the
254 log survival ratios were similar in the two solutions, which was also observed for *B.*
255 *subtilis* and *S. aureus.* These comparisons indicate that the air plasma jet has the same
256 high bactericidal effect in distilled water as in that in the nutrient solution. Thus, the air
257 plasma jet-induced bactericidal effect was not relevant to the nutrient components
258 included in the nutrient solution.
259 The inactivation exerted by the air plasma jet, which contained 80% N_2 and 20% O_2
260 molecules in the feed gas, was compared with the N_2-plasma-jet-induced results. Figure
261 8 shows the log survival ratios of *E. coli*, *B. subtilis*, and *S. aureus* suspended in nutrient

solutions irradiated with a N_2 plasma jet at 1 L/min. The intensity of the 337 nm UV associated with 2P(0,0) was 890 μW/cm^2, as measured with the same optical power meter as that used with the air plasma jet. The UV intensity was approximately five times higher than that emitted by the air plasma jet. In the case of the N_2 plasma jet, the log survival ratio of *E. coli* decreased from 0 to −0.8 when the irradiation time increased from 0 to 7 min. The log survival ratio of *B. subtilis* also decreased to −1 as the irradiation time increased. The log survival ratio of *S. aureus* remained unchanged from −0.3 with increased irradiation time. Comparing these results with those in Figs. 2−4, the air-plasma-jet-induced bactericidal effects were considerably higher than the N_2-plasma-jet-induced bactericidal effects, despite the N_2 plasma jet emitting a higher UV intensity than the air plasma jet. This suggests that the air-plasma-jet-induced bactericidal effects were not due to the UV emitted from the plasma. The results obtained are similar to those acquired from comparing the bactericidal effects induced by He and He/O_2 plasma jets [45,46]. The He plasma containing O_2 molecules in the feed gas showed a higher bactericidal effect, suggesting that the RONS generated with O_2 molecules in the gas play a crucial role in the level of bactericidal activity [45,46].

Figure 9 shows the variations in Fe, N, K, and P concentrations in plant nutrient solutions irradiated with a N_2 plasma jet at 1 L/min at the irradiation durations. The N concentration remained the same before irradiation as the irradiation time increased to 7 min, as opposed to the results of the air plasma jet (Fig. 6). This result suggests that the number of RONS generated in the air plasma jet was greater than that in the N_2 plasma jet. The Fe, K, and P concentrations did not change from those before irradiation as the irradiation time increased. This result is similar to that observed for the air plasma jet (Fig. 6), suggesting that the RONS generated in the air and N_2 plasma jets did not damage the nutrient components. Thus, the comparison between the N_2- and air-plasma-jet-induced results indicates that the higher bactericidal effect induced by the air plasma jet is

attributed predominantly to more RONS generated with O_2 molecules contained in the feed gas, which do not harm the nutrient components.

The PASs, that is, the RONS introduced in the nutrient solution by the air plasma jet, had a low bactericidal effect, as shown in Fig. 10. The PASs for *E. coli*, *B. subtilis*, and *S. aureus* were produced for 30 s, 20 s, and 7 min, respectively, with an air plasma jet at 1 L/min. Specifically, the irradiation times for producing PASs for *E. coli*, *B. subtilis*, and *S. aureus* were set to those required to inactivate the bacteria. The immersion times for each bacterium in the PASs were set to the duration required to inactivate each species. The log survival ratios of bacteria immersed in the PASs (red data) were considerably larger than those induced by the air plasma jet (blue data). This suggests that the PASs only minimally inactivated the bacteria suspended in the nutrient solution. Thus, the air-plasma-jet-induced inactivation of bacteria suspended in the nutrient solution cannot be explained only from the viewpoint of the RONS introduced in the nutrient solution. In summary, RONS, such as O, O_2^-, O_3, ·OH, and NO_x [45−51], from the air plasma jet on the nutrient solution surface would contribute to predominantly inactivating the bacteria suspended in the nutrient solution and would not damage the nutrient components.

4. Discussion

TWCEC-produced air plasma jet irradiation significantly inactivated the bacteria suspended in the nutrient solutions without reducing the nutrient components (Figs. 2–6). The air-plasma-jet-induced bactericidal effect observed in Fig. 7 differs from that induced by the submerged liquid plasma in air gas [25]. In the case of the submerged liquid plasma, the bactericidal effect of the plant nutrient solution was comparatively low in relation to that of distilled water. This implies that the bactericidal effect of the submerged liquid plasma was weakened or suppressed by the nutrient components included in the nutrient solution. This comparison suggests that the TWCEC-produced air plasma jet irradiation

314 proposed in this study is an effective means of inactivating bacteria suspended in plant
315 nutrient solutions.

316 The inactivation induced by the TWCEC-produced air plasma jet was compared to
317 that reported in the literature [27−31]. The inactivation of *E. coli*, at 3×10^3 CFU/mL/s,
318 which was defined by dividing 10^5 CFU/mL by 30 s, was compared with that exerted by
319 HEC-produced air plasma jets [27]. The HEC-produced air plasma jet reduced the log
320 survival of *E. coli* from 4 to 1 CFU/mL when the irradiation time increased from 0 to 50
321 s [27]. This suggests that 50 s of irradiation with the HEC-produced air plasma jet
322 inactivated the viable cell number by three orders of magnitude. Accordingly, the
323 inactivation of the HEC-produced air plasma jet was estimated at 2×10 CFU/mL/s,
324 which was substantially lower than that exerted by the TWCEC-produced air plasma jet
325 (Fig. 2(a)). The inactivation of *B. subtilis* (at 5×10^3 CFU/mL/s) was compared with that
326 of Ar-based plasma jets with O_2 and H_2O_2 vapors [30,31]. An Ar-based plasma jet with
327 3.59% O_2 reduced the log survival of *B. subtilis* from 6 CFU/mL to 2 CFU/mL as the
328 irradiation time increased from 0 s to 60 s [30]. A similar reduction in the log survival
329 number occurred in the case of an Ar-based plasma jet with H_2O_2 vapor [31]. This
330 suggests that the Ar-based plasma jets inactivated the viable cell number by three orders
331 of magnitude in 60 s by adding oxygen-based species. Hence, the inactivation induced by
332 the Ar-based plasma jets, at approximately 2×10 CFU/mL/s, was low compared to that
333 of the TWCEC-produced air plasma jet (Fig. 3(a)).

334 As shown in Fig. 4, the inactivation of *S. aureus* was estimated to occur at 2×10^2
335 CFU/mL/s, which was lower than that of the other types of bacteria used (Figs. 2 and 3).
336 This was compared with that exerted by RCEC-produced air plasma jets [28,29]. The
337 RCEC-produced air plasma jet reduced the survival of *S. aureus* from 20×10^7 to 2×10^7
338 CFU/mL as the irradiation time increased from 0 to 15 min [28,29]. This result suggests
339 that 15 min of irradiation with the RCEC-produced air plasma jet inactivated the viable

cell number by an order of magnitude. In other words, the inactivation of the RCEC-produced air plasma jet was estimated to occur at less than 1 CFU/mL/s, which was much lower than that exerted by the TWCEC-produced air plasma jet (Fig. 4(a)). Thus, TWCEC-produced air plasma jet irradiation is superior to the other methods and effective for inactivating bacteria suspended in nutrient solutions.

The majority of RONS introduced in solutions by plasma jets are reported to be long-lived species, such as hydrogen peroxides (H_2O_2), nitrite ions (NO_3^-), and nitrate ions (NO_2^-) [52], and short-lived species, such as hydroxyl radicals (·OH) [53,54]. Figure 11 shows the changes in the concentrations of H_2O_2, ·OH, NO_3^-, and NO_2^- introduced in the plant nutrient solution by air plasma jet irradiation at 1 L/min with the various irradiation times. The H_2O_2 concentration was determined by absorptiometry at a wavelength of 560 nm based on the peroxide-mediated oxidation of Fe^{2+} followed by the reaction of Fe^{3+} with xylenol orange [55,56]. The ·OH concentration was determined using the chemical probe method based on the 426 nm fluorescence of hydroxyterephthalic acid excited with 312 nm UV [53,54,57]. NO_3^- and NO_2^- concentrations were assessed using reduction and naphthyl ethylenediamine absorptiometry (WAK-NO3, Kyoritsu Chemical-Check Lab. Corp., Japan) and naphthyl ethylenediamine absorptiometry (WAK-NO2, Kyoritsu Chemical Check Lab. Corp., Japan), respectively, using the same portable multi-parameter water analyzer as that used to measure the Fe and P concentrations. At irradiation times of 0.3−0.5 min, the NO_3^- concentration was the greatest, followed by the NO_2^-, H_2O_2, and ·OH concentration in that order. These concentrations increased as the irradiation time was lengthened to 7 min, but the concentration order did not change. The concentrations of the air-plasma-jet-introduced RONS were considered to be small enough to inactivate the bacteria because they have a low bactericidal effect (Fig. 10). In addition, from the results shown in Fig. 6, the air-plasma-jet-introduced RONS did not damage the nutrient components in the nutrient solution. This implies that the RONS

366 introduced in the solution do not harm the growth of plants, which will be clarified in
367 future studies conducted under plant growth conditions.

368 The increase in the concentration of N induced by the air plasma jet (Fig. 6) has been
369 discussed in terms of the interactions between air plasma and water [47,58]. In the air
370 plasma jet, O and N radicals are generated through the dissociative reactions of O_2 and
371 N_2 molecules, respectively, due to electron impact [47]. The generated O and N radicals
372 chemically react with N_2 and O_2 molecules in the air plasma jet, respectively, producing
373 nitrogen oxides (NO_x) [47]. These nitrogen oxides chemically react with water, causing
374 the formation of nitrate ions (NO_3^-) and nitrite ions (NO_2^-) in the solution (Figs. 11(c)
375 and 11(d)). Thus, large numbers of RONS, such as NO_x generated by the air plasma jet,
376 contribute to the increased N concentration in the solution.

377

378 **5. Conclusion**

379 We clarified the bactericidal effects of TWCEC-produced air plasma jets on nutrient
380 solutions from the perspective of plasma-induced damage. The TWCEC-produced air
381 plasma jet directly irradiated the surface of the bacterial suspension. Air plasma jet
382 irradiation with a low gas flow rate sufficiently inactivated *E. coli*, *B. subtilis*, and *S.*
383 *aureus* suspended in nutrient solutions without reducing the nutrient concentrations. The
384 inactivation of the TWCEC-produced air plasma jet was greater than those of the plasma
385 jets produced by other types of electrode configurations. However, the plasma irradiation
386 time required to inactivate bacteria depended on the type of bacteria: *E. coli* and *B. subtilis*
387 were inactivated in 20–30 s, whereas *S. aureus* required 7 min for inactivation. The
388 inactivation of *E. coli* and *B. subtilis* was lowered by increasing the air gas flow rate, and
389 the inactivation of *S. aureus* was independent of this rate. This inactivation could be
390 attributed predominantly to a greater number of RONS impinging from the air plasma jet,
391 including O_2 molecules in the feed gas, onto the bacterial suspension surface, which

would not harm the nutrient components. This can be derived mainly from the following results: the PASs, that is, the RONS introduced in the nutrient solution by the air plasma jet, and the N_2 plasma jet without O_2 molecules in the feeding gas showed little inactivation ability of the bacteria suspended in the nutrient solution. These findings are important for a deeper understanding of the interactions between air plasma jets and plant nutrient solutions. TWCEC-produced air plasma jet irradiation provides a new perspective on improving the bactericidal effect of bacteria suspended in nutrient solutions without damaging the nutrient components in the solutions.

CRediT authorship contribution statement

Retsuo Kawakami: Conceptualization, Methodology, Data Curation, Resources, Formal analysis, Writing - Original Draft, Writing - Review & Editing, Project administration, Supervision. **Mutsumi Aihara:** Methodology, Investigation, Data Curation, Resources, Validation, Formal analysis, Writing - Review & Editing, Supervision. **Takuto Izumi:** Methodology, Investigation, Data Curation, Validation, Formal analysis, Writing - Review & Editing. **Akihiro Shirai:** Methodology, Investigation, Data Curation, Resources, Validation, Formal analysis, Writing - Review & Editing, Supervision. **Takashi Mukai:** Writing - Review & Editing, Supervision, Funding acquisition.

Acknowledgments

Parts of this study were supported by Japan Power Academy: Grant-in-Aid for Exploratory Research No. o2021-H10a. The authors would like to appreciate Mr. Kousuke Takagi, Mr. Takumi Matsumura, Mr. Kazuki Nomoto at the Department of Science and Engineering at Tokushima University, and Miss. Tomona Urakami at the Department of Bioscience and bioindustry at Tokushima University for partially

supporting the bacterial inactivation experiments. The authors would also like to thank Dr. Tomoyuki Ueki at Tokushima University for his assistance with the SEM observation of bacteria. Furthermore, the authors would like to thank Editage (www.editage.com) for English language editing.

Conflict of Interest

The authors declare no conflict of interest.

Data Availability Statement

The data that support the findings of this study are available from the corresponding author upon reasonable request.

444 **References**

445 [1] A. B. Raymond, A. Alpha, T. Ben-Ari, B. Daviron, T. Nesme, G. Tetart, Systemic risk
446 and food security. Emerging trends and future avenues, Glob. Food Sec. **29** (2021)
447 100547:1−9, https://doi.org/10.1016/j.gfs.2021.100547.
448 [2] J. J. L. Westerveld, M. J. C. van den Homberg, G. G. Nobre, D. L. J. van den Berg, A.
449 D. Teklesadik, S. M. Stuit, Forecasting transitions in the state of food security with
450 machine learning using transferable features, Sci. Total Environ. **786** (2021) 147366:1−15,
451 https://doi.org/10.1016/j.scitotenv.2021.147366.
452 [3] H. Azadi, S. M. Moghaddam, S. Burkart, H. Mahmoudi, S. V. Passel, A. Kurban, D.
453 L. Carr, Rethinking resilient agriculture: from climate-smart agriculture to vulnerable-
454 smart agriculture, J. Clean. Prod. **319** (2021) 138602:1−10,
455 https://doi.org/10.1016/j.jclepro.2021.128602.
456 [4] A. Mekonnen, A. Tessema, Z. Ganewo, A. Haile, Climate change impacts on
457 household food security and farmers adaptation strategies, J. Agri. Food Res. **6** (2021)
458 100197:1−9, https://doi.org/10.1002/fes3.266.
459 [5] C. P. Leisner, Review: climate change impacts on food security- focus on perennial
460 cropping systems and nutritional value, Plant Sci. **293** (2020) 110412:1−7,
461 https://doi.org/10.1016/j.plantsci.2020.110412.
462 [6] G. Xydis, D. Strasszer, D. D. Avgoustaki, E. Nanaki, Mass deployment of plant
463 factories as source of load flexibility in the grid under an energy-food nexus. A
464 technoeconomics-based comparison, Sustain. Energy Technol. Assess. **47** (2021)
465 101431:1−10, https://doi.org/10.1016/j.seta.2021.101431.
466 [7] L. Kun, F. Hui, Z. Zhi-rong, C. Rui-feng, Optimization of rhizosphere cooling airflow
467 for microclimate regulation and its effects on lettuce growth in plant factory, J. Integr.
468 Agric. **20** (2021) 2680−2695, https://doi.org/10.1016/S2095-3119(20)63382-2.
469 [8] J. W. Huebbers, J. F. Buyel, On the verge of the market – plant factories for the

automated and standardized production of biopharmaceuticals, Biotechnol. Adv. **46** (2021) 107681:1−18, https://doi.org/10.1016/j.biotechadv.2020.107681.

[9] R. He, Y. Zhang, S. Song, W. Su, Y. Hao, H. Liu, UV-A and FR irradiation improves growth and nutritional properties of lettuce grown in an artificial light plant factory, Food Chem. **345** (2021) 128727:1−9, https://doi.org/10.1016/j.foodchem.2020.128727.

[10] L. Graamans, M. Tenpierik, A. van den Dobbelsteen, C. Stanghellini, Plant factories: reducing energy demand at high internal heat loads through facade design, Appl. Energ. **262** (2020) 114544:1−19, https://doi.org/10.1016/j.apenergy.2020.114544.

[11] G. A. Xydis, S. Liaros, D. Avgoustaki, Small scale plant factories with artificial lighting and wind energy microgeneration: a multiple revenue stream approach, J. Clean. Prod. **255** (2020) 120227:1−12, https://doi.org/10.1016/j.jclepro.2020.120227.

[12] M. R. Talukder, M. Asaduzzaman, H. Tanaka, T. Asao, Light-emitting diodes and exogenous amino acids application improve growth and yield of strawberry plants cultivated in recycled hydroponics, Sci. Hortic. **239** (2018) 93−103, https://doi.org/10.1016/j.scienta.2018.05.033.

[13] L. Settanni, A. Miceli, N. Francesca, M. Cruciata, G. Moschetti, Microbiological investigation of *Raphanus sativus* L. grown hydroponically in nutrient solutions contaminated with spoilage and pathogenic bacteria, Int. J. Food Microbiol. **160** (2013) 344−352, https://doi.org/10.1016/j.ijfoodmicro.2012.11.011.

[14] A. Tsunedomi, K. Miyawaki, A. Masamura, M. Nakahashi, K. Mawatari, T. Shimohata, T. Uebanso, Y. Kinouchi, M. Akutagawa, T. Emoto, A. Takahashi, UVA-LED device to disinfect hydroponic nutrient solution, J. Med. Invest. **65** (2018) 171−176, https://doi.org/10.2152/jmi.65.171.

[15] Y. W. Liu, C. K. Huang, Effects of the circulation pump type and ultraviolet sterilization on nutrient solutions and plant growth in plant factories, HortTechnology **29** (2019) 189−198, https://doi.org/10.21273/HORTTECH04244-18.

[16] J. P. Albano, W. B. Miller, Photodegradation of FeDTPA in nutrient solutions. I. Effects of irradiance, wavelength, and temperature, HortScience **36** (2001) 313−316, https://doi.org/10.21273/HORTSCI.36.2.313.

[17] M. Keidar, K. D. Weltmann, S. Macheret, Fundamentals and applications of atmospheric pressure plasmas, J. Appl. Phys. **130** (2021) 080401:1−4, https://doi.org/10.1063/5.0065750.

[18] M. Dezest, A. L. Bulteau, D. Quinton, L. Chavatte, M. L. Bechec, J. P. Cambus, S. Arbault, A. Nègre-Salvayre, F. Clément, S. Cousty, Oxidative modification and electrochemical inactivation of *Escherichia coli* upon cold atmospheric pressure plasma exposure, PLoS ONE **12** (2017) e0173618: 1−18, https://doi.org/10.1371/journal.pone.0173618.

[19] T. Homolid, V. Prukner, A. Artemenko, J. Hanus, O. Kylian, M. Simek, Direct treatment of pepper (*Capsicum annuum* L.) and melon (*Cucumis melo*) seeds by amplitude-modulated dielectric barrier discharge in air, J. Appl. Phys. **129** (2021) 193303:1−15, https://doi.org/10.1063/5.0039165.

[20] S. Saremmezhad, M. Soltani, A. Faraji, A. A. Hayaloglu, Chemical changes of food constituents during cold plasma processing: a review, Food Res. Int. **147** (2021) 110552:1−14, https://doi.org/10.1016/j.foodres.2021.110552.

[21] E. Bormashenko, Y. Bormashenko, I. Legchenkova, N. M. Eren, Cold plasma hydrophilization of soy protein isolate and milk protein concentrate enables manufacturing of surfactant-free water suspensions. Part I: hydrophilization of food powders using cold plasma, Innov. Food Sci. Emerg. Technol. **72** (2021) 102759:1−7, https://doi.org/10.1016/j.ifset.2021.102759.

[22] A. Niveditha, R. Pandiselvam, V. A. Prasath, S. K. Singh, K. Gul, A. Kothakota, Application of cold plasma and ozone technology for decontamination of Escherichia coli in foods- a review, Food Control **130** (2021) 108338:1−11,

https://doi.org/10.1016/j.foodcont.2021.108338.

[23] S. Y. Lee, J. In, M. S. Chung, S. C. Min, Microbial decontamination of particulate food using a pilot-scale atmospheric plasma jet treatment system, J. Food Eng. **294** (2021) 110436:1−8, https://doi.org/10.1016/j.jfoodeng.2020.110436.

[24] B. Pang, Z. Liu, S. Wang, Y. Gao, H. Zhang, F. Zhang, X. Tantai, D. Xu, D. Liu, M. G. Kong, Discharge mode transition in a He/Ar atmospheric pressure plasma jet and its inactivation effect against tumor cells in vitro, J. Appl. Phys. **130** (2021) 153301:1−12, https://doi.org/10.1063/5.0063135.

[25] S. Yasui, S. Seki, R. Yoshida, K. Shoji, H. Terazoe, Sterilization of *Fusarium oxysporum* by treatment of non-thermalequilibrium plasma, Jpn. J. Appl. Phys. **55** (2016) 01AB01:1−5, http://doi.org/10.7567/JJAP.55.01AB01.

[26] R. Kawakami, Y. Yoshitani, K. Mitani, M. Niibe, Y. Nakano, C. Azuma, T. Mukai, Effects of air-based nonequilibrium atmospheric pressure plasma jet treatment on characteristics of polypropylene film surfaces, Appl. Surf. Sci. **509** (2020) 144910:1−10, https://doi.org/10.1016/j.apsusc.2019.144910.

[27] W. S. Kang, Y. C. Hong, Y. B. Hong, J. H. Kim, H. S. Uhm, Atmospheric-pressure cold plasma jet for medical applications, Surf. Coat. Technol. **205** (2010) S418−S421, https://doi.org/10.1016/j.surfcoat.2010.08.138.

[28] P. Thana, A. Wijaikhum, P. Poramapijitwat, C. Kuensaen, J. Meerak, A. Ngamjarurojana, S. Sarapirom, D. Boonyawan, A compact pulse-modulation cold air plasma jet for the inactivation of chronic wound bacteria: development and characterization, Heliyon **5** (2019) e02455:1−11, https://doi.org/10.1016/j.heliyon.2019.e02455.

[29] P. Thanaa, C. Kuensaena, P. Poramapijitwat, S. Sarapirom, L. Yu, D. Boonyawan, A compact pulse-modulation air plasma jet for the inactivation of chronic wound bacteria: bactericidal effect & host safety, Surf. Coat. Technol. **400** (2020) 126229:1−10,

548 https://doi.org/10.1016/j.surfcoat.2020.126229.
549 [30] S. Deng, C. Cheng, G. Ni, Y. Meng, H. Chen, *Bacillus subtilis* devitalization
550 mechanism of atmosphere pressure plasma jet, Curr. Appl. Phys. **10** (2010) 1164−1168,
551 https://doi.org/10.1016/j.cap.2010.02.004.
552 [31] D. S. Xi, C. Cheng, N. G. Hua, M. Y. Dong, C. Hua, The interaction of an
553 atmospheric pressure plasma jet using argon or argon plus hydrogen peroxide vapor
554 addition with *bacillus subtilis*, Chin. Phys. B **19** (2010) 10523:1−6,
555 https://doi.org/10.1088/1674-1056/19/10/105203.
556 [32] M. He, T. Wu, S. Pan, X. Xu, Antimicrobial mechanism of flavonoids against
557 *Escherichia coli* ATCC25922 by model membrane study, Appl. Surf. Sci. **305** (2014)
558 515−521, https://doi.org/10.1016/j.apsusc.2014.03.125.
559 [33] E. Rochima, N. Sekar, I. D. Buwono, E. Afrianto, R. I. Pratama, Isolation and
560 characterization of collagenase from *Bacillus subtilis* (Ehrenberg, 1835); ATCC 6633 for
561 degrading fish skin collagen waste from Cirata reservoir, Indonesia, Aquat. Procedia **7**
562 (2016) 76−84, https://doi.org/10.1016/j.aqpro.2016.07.010.
563 [34] L. Zhang, H. Ma, S. Wang, Pasteurization mechanism of *S. aureus* ATCC 25923 in
564 walnut shells using radio frequency energy at lab level, LWT - Food Sci. Technol. **143**
565 (2021) 111129:1−7, https://doi.org/10.1016/j.lwt.2021.111129.
566 [35] H. Donya, T. A. Taha, A. Alruwaili, I. B. I. Tomsah, M. Ibrahim, Micro-structure and
567 optical spectroscopy of PVA/iron oxide polymer nanocomposite, J. Mater. Res. Technol.
568 **9** (2020) 9189−9194, https://doi.org/10.1016/j.jmrt.2020.06.040.
569 [36] K. Granholm, T. Sokalski, A. Lewenstam, A. Ivaska, Ion-selective electrodes in
570 potentiometric titrations; a new method for processing and evaluating titration data, Anal.
571 Chim. Acta **888** (2015) 36−43, https://doi.org/10.1016/j.aca.2015.05.056.
572 [37] A. E. Liana, C. P. Marquis, C. Gunawan, J. J. Gooding, R. Amal, T4 bacteriophage
573 conjugated magnetic particles for *E. coli* capturing: influence of bacteriophage loading,

574 temperature and tryptone, Colloids Surf. B Biointerfaces **151** (2017) 47−57,
575 https://doi.org/10.1016/j.colsurfb.2016.12.009.
576 [38] J. Shi, F. Zhang, S. Wu, Z. Guo, X. Huang, X. Hu, M. Holmes, X. Zou, Noise-free
577 microbial colony counting method based on hyperspectral features of agar plates, Food
578 Chem. **274** (2019) 925−932, https://doi.org/10.1016/j.foodchem.2018.09.058.
579 [39] M. S. Jang, S. Sahastrabuddhe, C. H. Yun, S. H. Han, J. S. Yang, Serum bactericidal
580 assay for the evaluation of typhoid vaccine using a semi-automated colony-counting
581 method, Microb. Pathog. **97** (2016) 19−26,
582 http://dx.doi.org/10.1016/j.micpath.2016.05.013.
583 [40] A. H. Basher, A. A. H. Mohamed, Laminar and turbulent flow modes of cold
584 atmospheric pressure argon plasma jet, J. Appl. Phys. **123** (2018) 193302:1−9,
585 https://doi.org/10.1063/1.5012087.
586 [41] Y. Yang, H. Wang, H. Zhou, Z. Hu, W. Shang, Y. Rao, H. Peng, Y. Zheng, Q. Hu, R.
587 Zhang, H. Luo, X. Ra, Protective Effect of the golden staphyloxanthin biosynthesis
588 pathway on Staphylococcus aureus under cold atmospheric plasma treatment, Appl.
589 Environ. Microbiol. **86** (2020) e01998-19:1−9, https://doi.org/10.1128/AEM.01998-19.
590 [42] A. Clauditz, A. Resch, K. P. Wieland, A. Peschel, F. Gotz, Staphyloxanthin plays a
591 role in the fitness of Staphylococcus aureus and its ability to cope with oxidative stress,
592 Infect. Immun. **74** (2006) 4950−4953, https://doi.org/10.1128/IAI.00204-06.
593 [43] L. Han, S. Patil, D. Boehm, V. Milosavljevic, P. J. Cullen, P. Bourke, Mechanisms of
594 inactivation by high-voltage atmospheric cold plasma differ for *Escherichia coli* and
595 *Staphylococcus aureus*, Appl. Environ. Microbiol. **82** (2016) 450−458,
596 https://doi.org/10.1128/AEM.02660-15.
597 [44] R. L. Walker, I. G. Burns, J. Moorby, Responses of plant growth rate to nitrogen
598 supply: a comparison of relative addition and N interruption treatments, J. Exp. Bot. **52**
599 (2001) 309−317, https://doi.org/10.1093/jexbot/52.355.309.

[45] J. L. Hobman, P. A. Lund, C. J. Kershaw, G. A. Hidalgo-Arroyo, C. W. Penn, X. T. Deng, J. L. Walsh, M. G. Kong, Probing bactericidal mechanisms induced by cold atmospheric plasmas with *Escherichia coli* mutants, Appl. Phys. Lett. **90** (2007) 073902:1−3, https://doi.org/10.1063/1.2458162.

[46] M. Dezest, A. L. Bulteau, D. Quinton, L. Chavatte, M. L. Bechec, J. P. Cambus, S. Arbault, A. N. Salvayre, F. Clement, S. Cousty, Oxidative modification and electrochemical inactivation of *Escherichia coli* upon cold atmospheric pressure plasma exposure, PLoS One **12** (2017) e0173618:1−18, https://doi.org/10.1371/journal.pone.0173618.

[47] A. Khlyustova, C. Labay, Z. Machala, M. P. Ginebra, C. Canal, Important parameters in plasmas jets for the production of RONS in liquids for plasma medicine; a brief review, Front. Chem. Sci. Eng. **13** (2019) 238−252, https://doi.org/10.1007/s11705-019-1801-8.

[48] R. Zhou, R. Zhou, P. Wang, Y. Xian, A. Mai-Prochnow, X. Lu, P. J. Cullen, K. Ostrikov, K. Bazaka, Plasma-activated water: Generation, origin of reactive species and biological applications, J. Phys. D: Appl. Phys. **53** (2020) 303001:1−28, https://doi.org/10.1088/1361-6463/ab81cf.

[49] S. Ikawa, K. Kitano, S. Hamaguchi, Effects of pH on bacterial inactivation in aqueous solutions due to low-temperature atmospheric pressure plasma application, Plasma Process. Polym. **7** (2010) 33−42, https://doi.org/10.1002/ppap.200900090.

[50] K. Shimada, K. Takashima, Y. Kimura, K. Nihei, H. Konishi, T. Kaneko, Humidification effect of air plasma effluent gas on suppressing conidium germination of a plant pathogenic fungus in the liquid phase, Plasma Process Polym. **17** (2020) e190000:1−15, https://doi.org/10.1002/ppap.201900004.

[51] Q. Wang, D. Salvi, Evaluation of plasma-activated water (PAW) as a novel disinfectant: effectiveness on *Escherichia coli* and *Listeria innocua*, physicochemical properties, and storage stability, LWT - Food Sci. Technol. **149** (2021) 111847:1−9,

626 https://doi.org/10.1016/j.lwt.2021.111847.
627 [52] K. Ogawa, J. S. Oh, N. Gaur, S. H. Hong, H. Kurita, A. Mizuno, A. Hatta, R. D.
628 Short, M. Ito, E. J. Szili, Modulating the concentration of reactive oxygen and nitrogen
629 species and oxygen in water with helium and argon gas and plasma jet, Jpn. J. Appl. Phys.
630 58 (2019) SAAB01:1−9, https://doi.org/10.7567/1347-4065/aaea6b.
631 [53] A. Tani, Y. Ono, S. Fukui, S. Ikawa, K. Kitano, Free radicals induced in aqueous
632 solution by non-contact atmospheric-pressure cold plasma, Appl. Phys. Lett. 100 (2012)
633 254103:1−3, https://doi.org/10.1063/1.4729889.
634 [54] S. Kanazawa, H. Kawano, S. Watanabe, T. Furuki, S. Akamine, R. Ichiki, T. Ohkubo,
635 M. Kocik, J. Mizeraczyk, Observation of OH radicals produced by pulsed discharges on
636 the surface of a liquid, Plasma Sources Sci. Technol. 20 (2011) 034010:1−8,
637 https://doi.org/10.1088/0963-0252/20/3/034010.
638 [55] A. Shirai, K. Kawasaka, K. Tsuchiya, Antimicrobial action of phenolic acids
639 combined with violet 405-nm light for disinfecting pathogenic and spoilage fungi, J.
640 Photochem. Photobiol. B: Biol. 229 (2022) 112411:1−8,
641 https://doi.org/10.1016/j.jphotobiol.2022.112411.
642 [56] Z. Y. Jiang, A. C. S. Woollard, S. P. Wolff, Hydrogen peroxide production during
643 experimental protein glycation, FEBS 268 (1990) 69−71, https://doi.org/10.1016/0014-
644 5793(90)80974-n.
645 [57] T. Hirakawa, K. Yawata, Y. Nosaka, Photocatalytic reactivity for O2•− and OH•
646 radical formation in anatase and rutile TiO2 suspension as the effect of H2O2 addition,
647 Appl. Catal. A: Gen. 325 (2007) 105−111, https://doi.org/10.1016/j.apcata.2007.03.015.
648 [58] R. Thirumdas, A. Kothakota, U. Annapure, K. Siliveru, R. Blundell, R. Gatt, V. P.
649 Valdramidis, Plasma activated water (PAW): chemistry, physico-chemical properties,
650 applications in food and agriculture, Trends Food Sci. Tech. **77** (2018) 21−31,
651 https://doi.org/10.1016/j.tifs.2018.05.007.

Figure captions:

Figure 1. (a) Schematic drawing of the experimental arrangement for disinfecting a plant nutrient solution including bacteria with an air plasma jet. Photographs of (b) the setup and (c) the air plasma jet in contact with the solution.

Figure 2. (a) The log survival ratio of *E. coli* suspended in a plant nutrient solution irradiated with the air plasma jet at 1 L/min, as a function of irradiation time. (b) Comparison between the log survival ratios of *E. coli* suspended in the solutions irradiated for 30 s with air plasma jets at 1, 3, and 5 L/min. The different letters shown in the figures signify statistically significant differences, P-values < 0.05, as estimated by the Tukey-Kramer test. The same letters shown in the figures mean no significant differences.

Figure 3. (a) The log survival ratios of *B. subtilis* suspended in a plant nutrient solution irradiated with the air plasma jet at 1 L/min, as a function of irradiation time. (b) Comparison between the log survival ratios of *B. subtilis* suspended in the solutions irradiated for 20 s with air plasma jets at 1, 3, and 5 L/min. The different letters shown in the figures signify statistically significant differences, P-values < 0.05, as estimated by the Tukey-Kramer test. The same letters shown in the figures mean no significant differences.

Figure 4. (a) The log survival ratios of *S. aureus* suspended in a plant nutrient solution irradiated with the air plasma jet at 1 L/min, as a function of irradiation time. (b) Comparison between the log survival ratios of *S. aureus* suspended in the solutions irradiated for 7 min with air plasma jets at 1, 3, and 5 L/min. The different letters shown in the figures signify statistically significant differences, P-values < 0.05, as estimated by the Tukey-Kramer test. The same letters shown in the figures mean no significant

678 differences.

679

680 **Figure 5.** (a) SEM images of *E. coli* before and after irradiating the bacterial suspension
681 with the air plasma jet at 1 L/min for 30 s. (b) SEM images of *B. subtilis* before and after
682 irradiating the bacterial suspension with the air plasma jet for 20 s. (c) SEM images of *S.*
683 *aureus* before and after irradiating the bacterial suspension with the air plasma jet for 7
684 min. The arrows shown in the figures correspond to the portions of plasma-induced
685 damage.

686

687 **Figure 6.** Fe, N, K, and P content concentrations in a plant nutrient solution irradiated
688 with the air plasma jet at 1 L/min, as a function of irradiation time.

689

690 **Figure 7.** Comparisons between the log survival ratios of (a) *E. coli*, (b) *B. subtilis*, and
691 (c) *S. aureus* suspended in distilled water and plant nutrient solutions irradiated with the
692 air plasma jet at 1 L/min for 30 s, 20 s, and 7 min, respectively. The abbreviation, n. s.,
693 shown in the figures signifies no significant differences, as estimated by the two-tailed
694 and unpaired t-test.

695

696 **Figure 8.** The log survival ratios of (a) *E. coli*, (b) *B. subtilis*, and (c) *S. aureus* suspended
697 in plant nutrient solutions irradiated with a N_2 plasma jet at 1 L/min, as a function of
698 irradiation time. The different letters shown in the figures signify statistically significant
699 differences, P-values < 0.05, as estimated by the Tukey-Kramer test. The same letters
700 shown in the figures mean no significant differences.

701

702 **Figure 9.** Fe, N, K, and P content concentrations in a plant nutrient solution irradiated
703 with a N_2 plasma jet at 1 L/min, as a function of irradiation time.

Figure 10. The log survival ratios of (a) *E. coli*, (b) *B. subtilis*, and (c) *S. aureus* suspended in PASs produced for 30 s, 20 s, and 7 min with the air plasma jet at 1 L/min, respectively. Their immersion times of bacteria in the PASs are the same as those required to inactivate the bacteria with the air plasma jet, respectively. The blue-colored data in the figures correspond to the results of *E. coli*, *B. subtilis*, and *S. aureus* suspended in the nutrient solution irradiated for 30 s, 20 s, and 7 min with the air plasma jet, respectively. The symbol, ***, shown in the figures corresponds to a P-value < 0.001, as estimated by the two-tailed and unpaired t-test.

Figure 11. Concentrations of (a) H_2O_2, (b) ·OH, (c) NO_3^-, and (d) NO_2^- generated in a plant nutrient solution by the air plasma jet irradiation at 1 L/min, as a function of irradiation time.

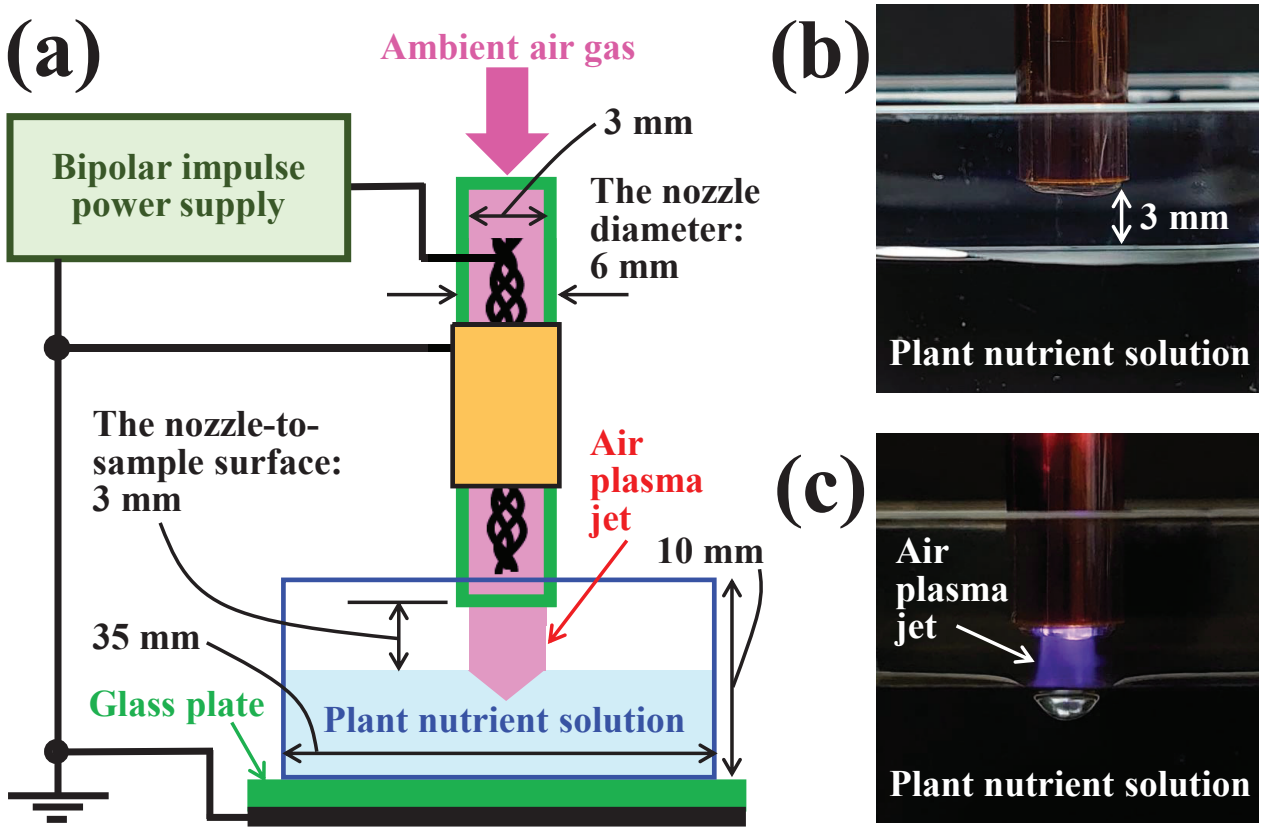

Figure 1. R. Kawakami *et al.*

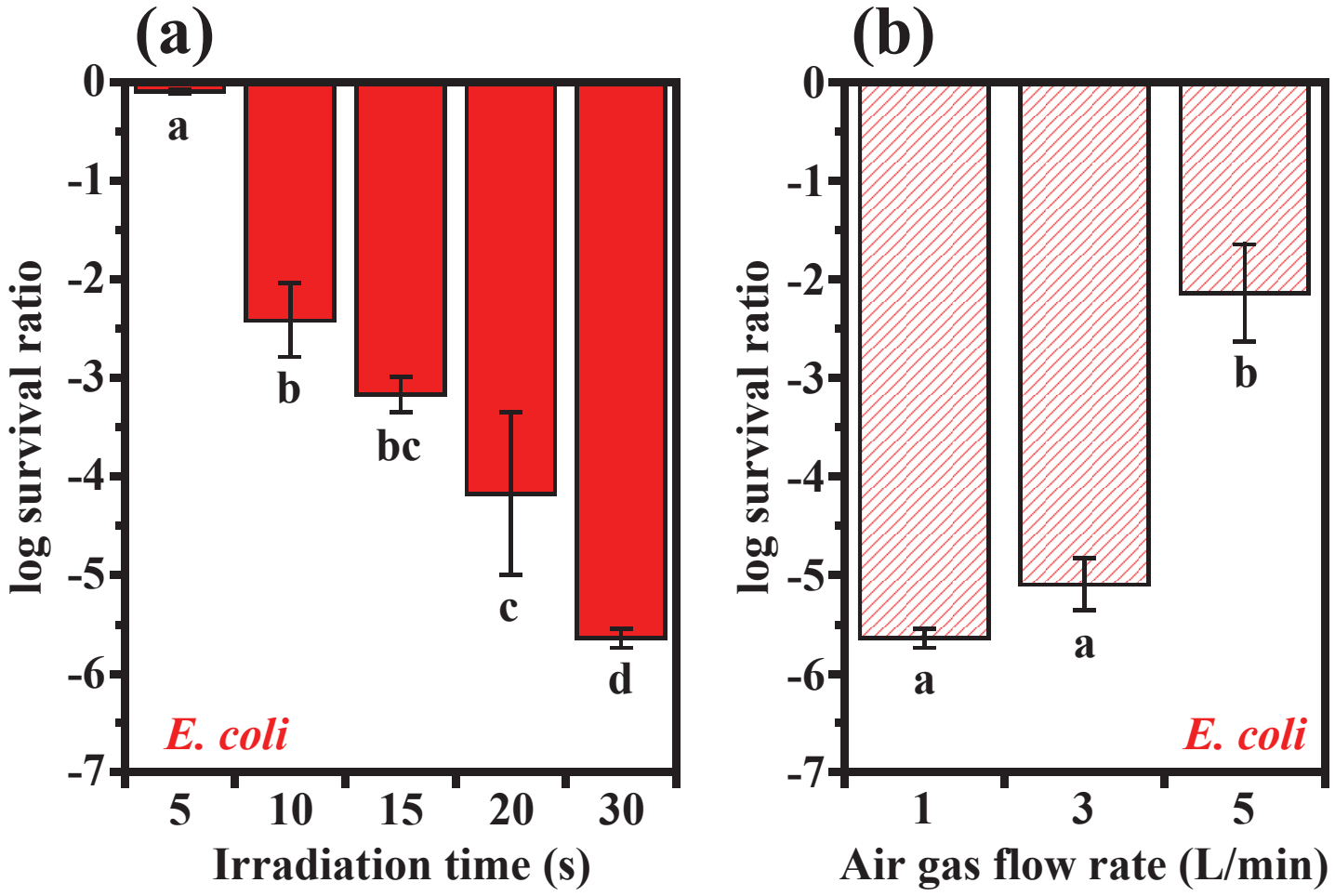

Figure 2. R. Kawakami *et al*.

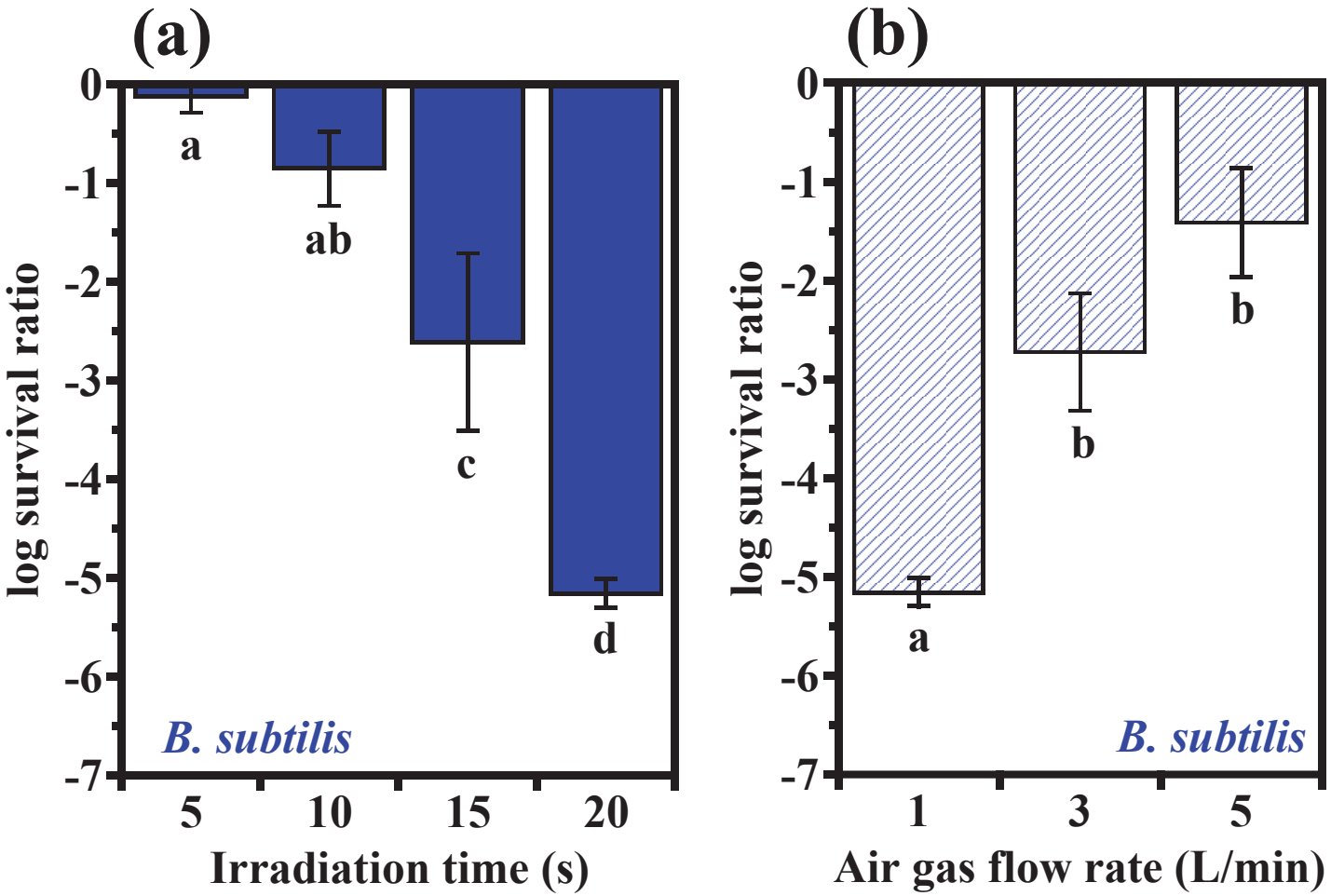

Figure 3. R. Kawakami *et al*.

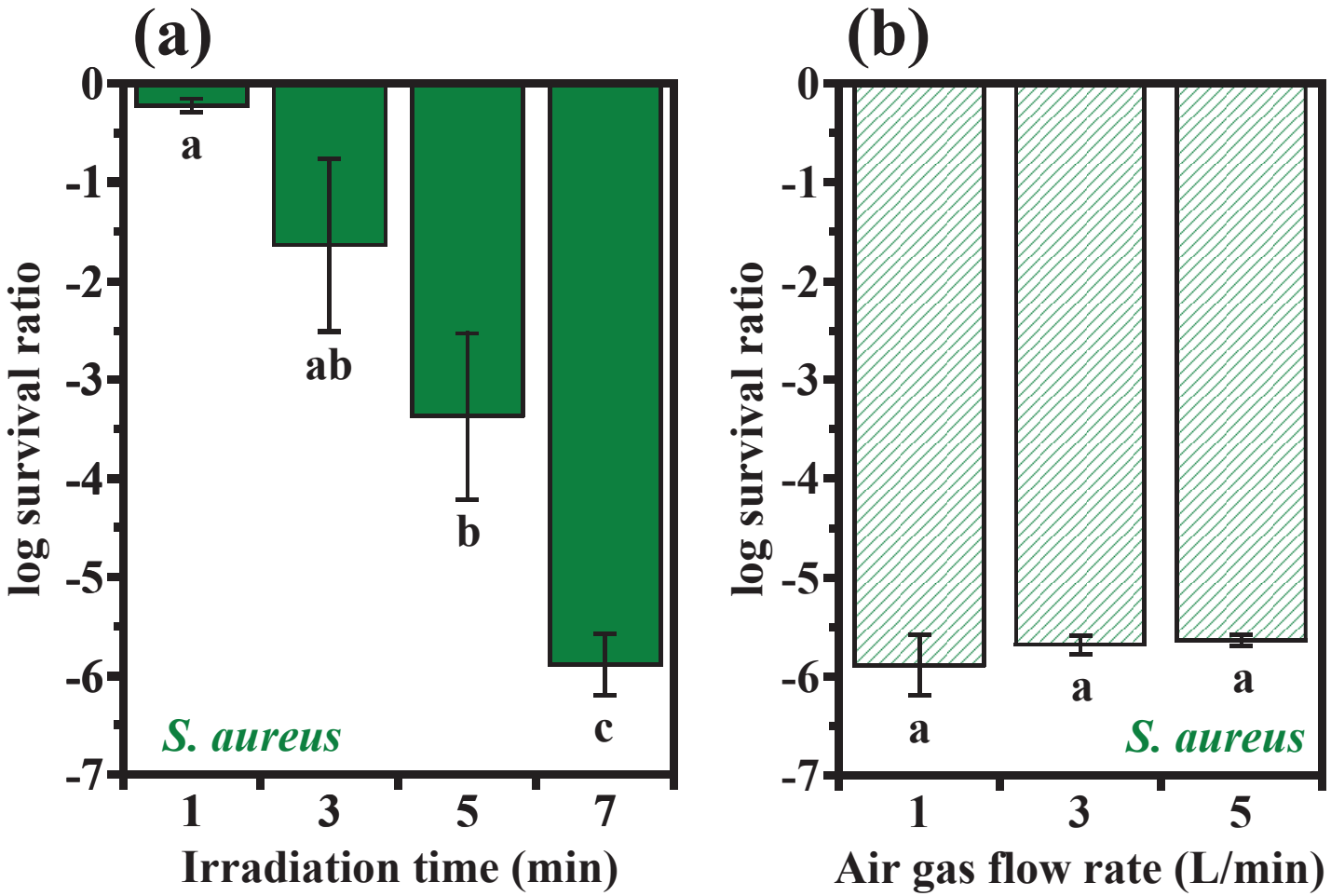

Figure 4. R. Kawakami *et al*.

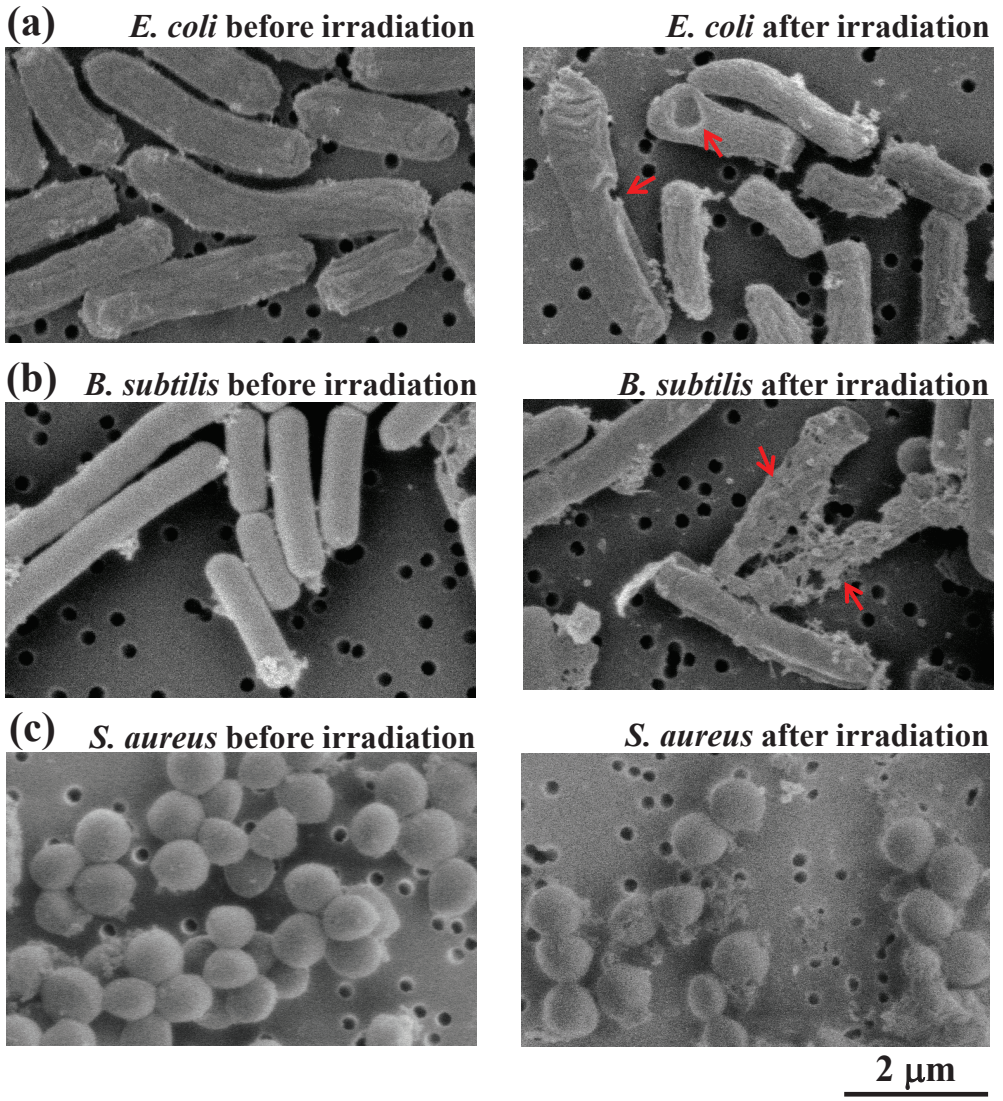

Figure 5. R. Kawakami *et al*.

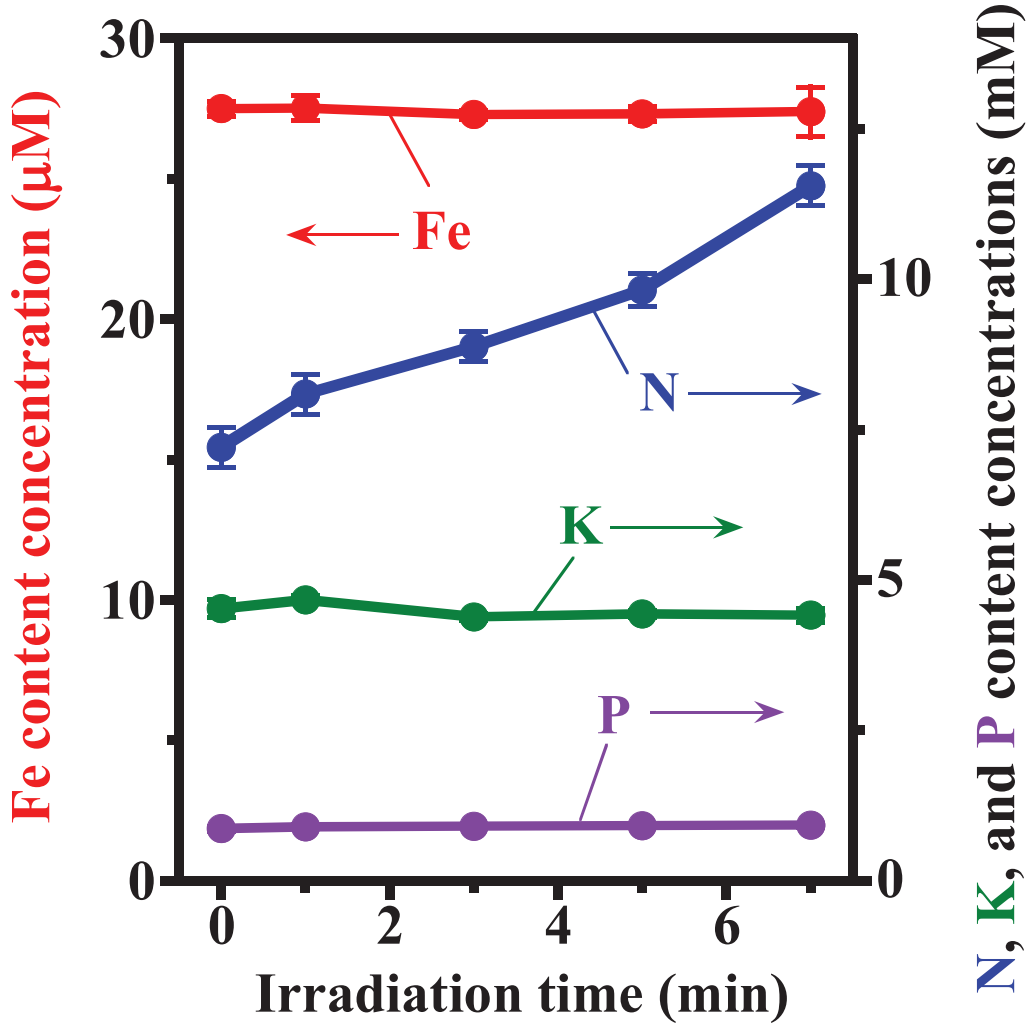

Figure 6. R. Kawakami *et al.*

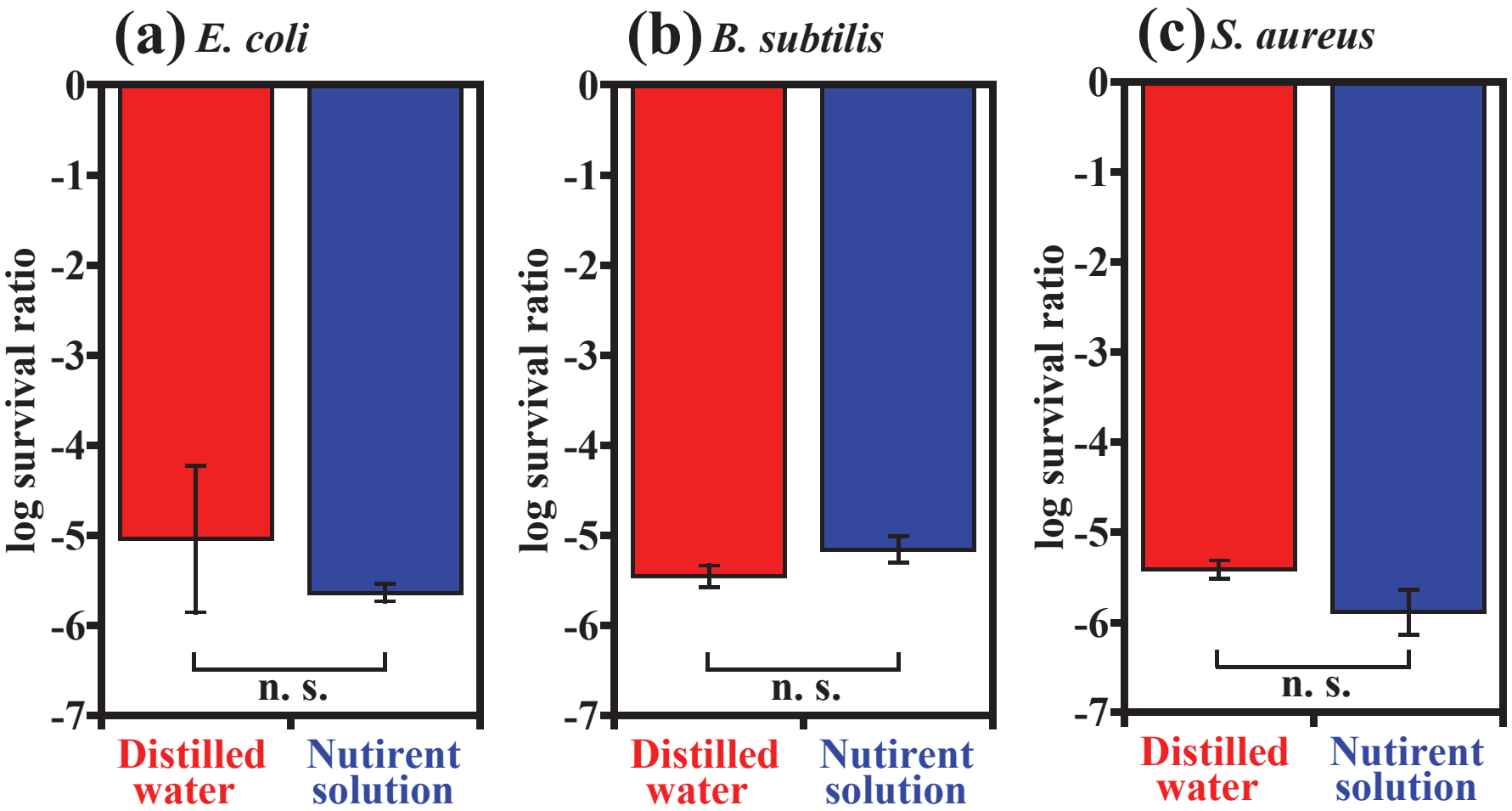

Figure 7. R. Kawakami *et al*.

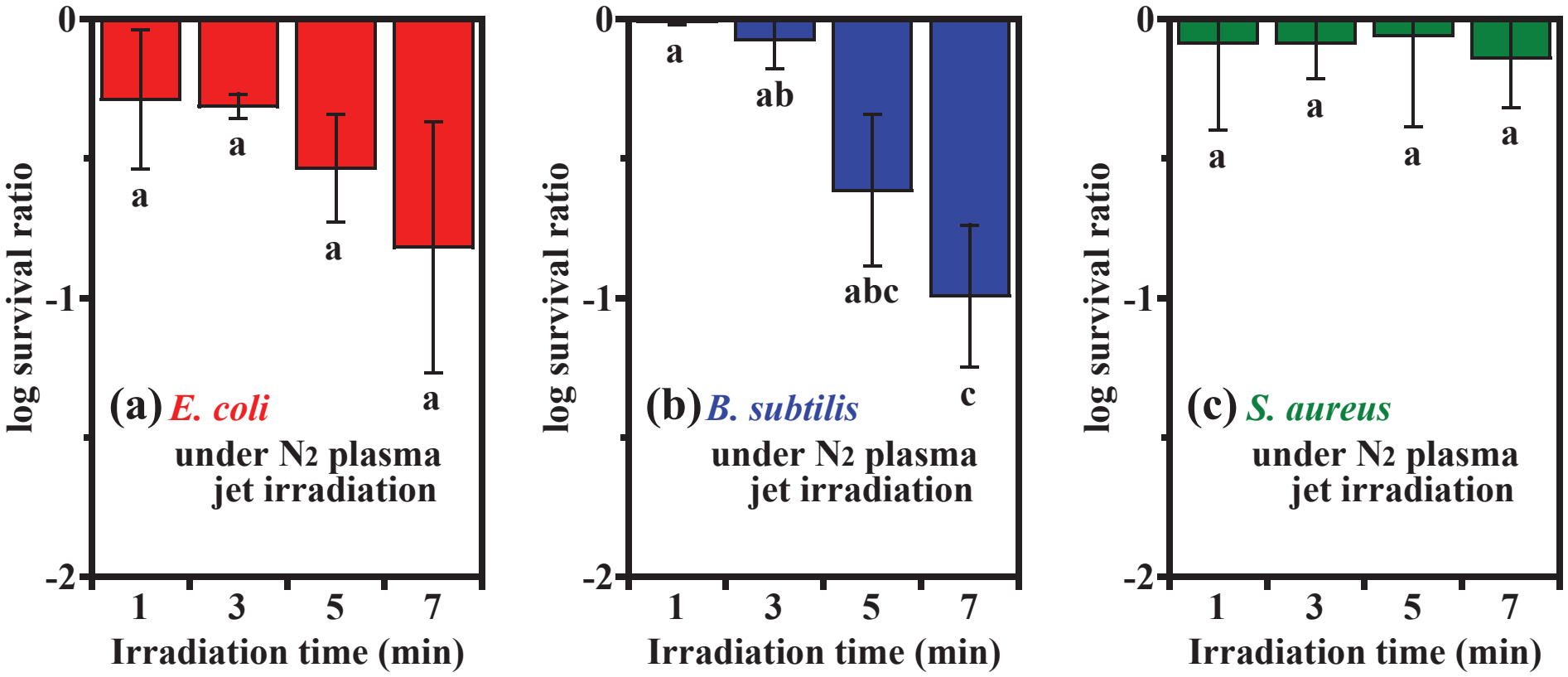

Figure 8. R. Kawakami *et al.*

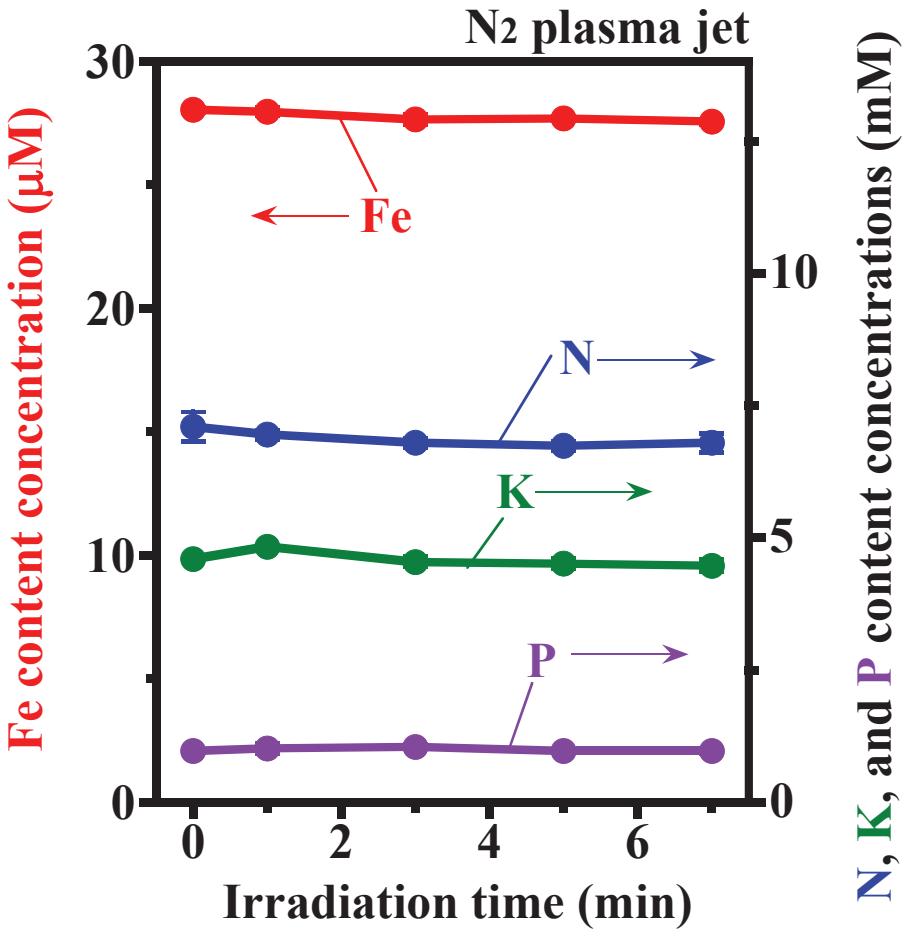

Figure 9. R. Kawakami *et al.*

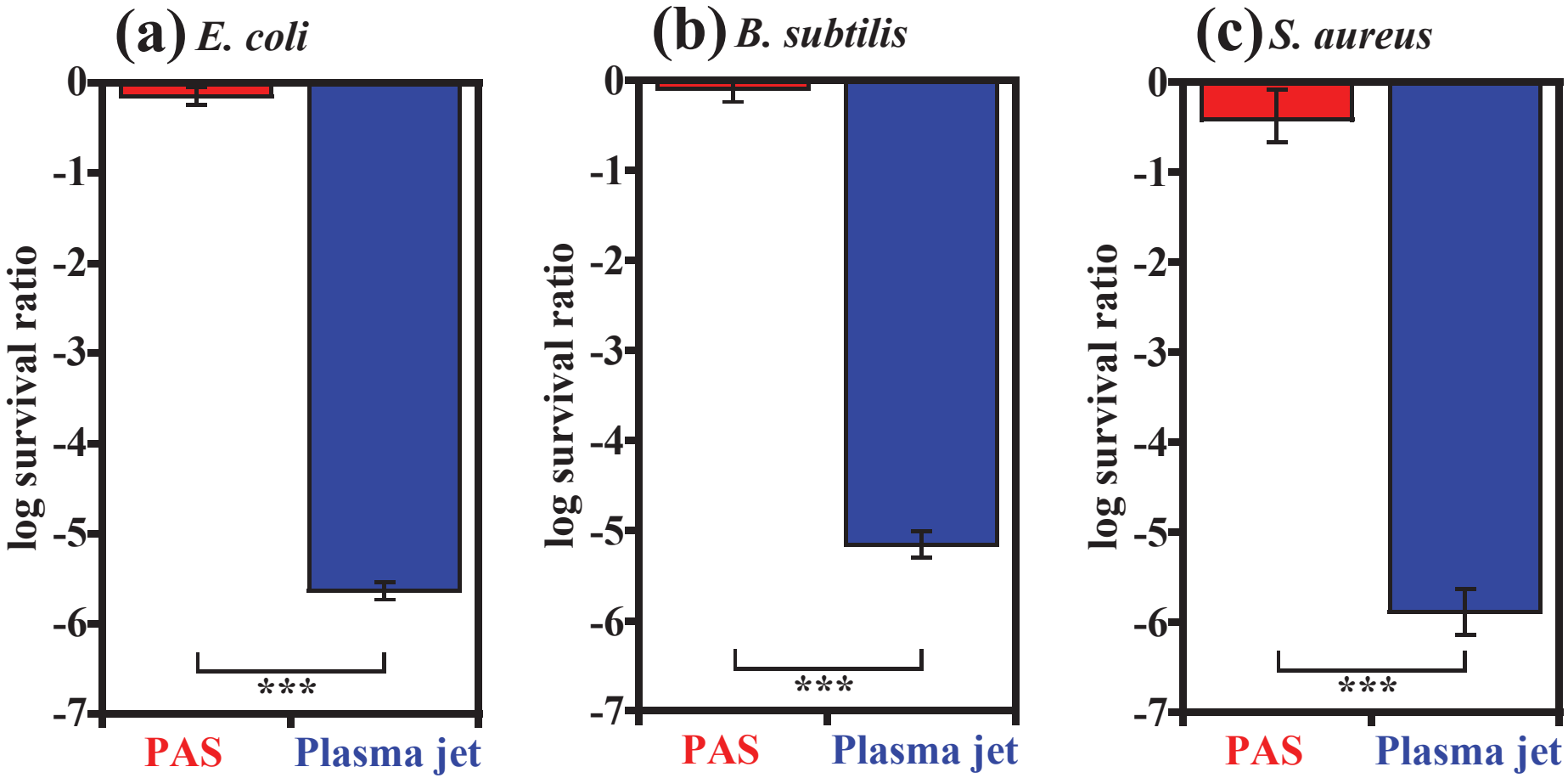

Figure 10. R. Kawakami *et al*.

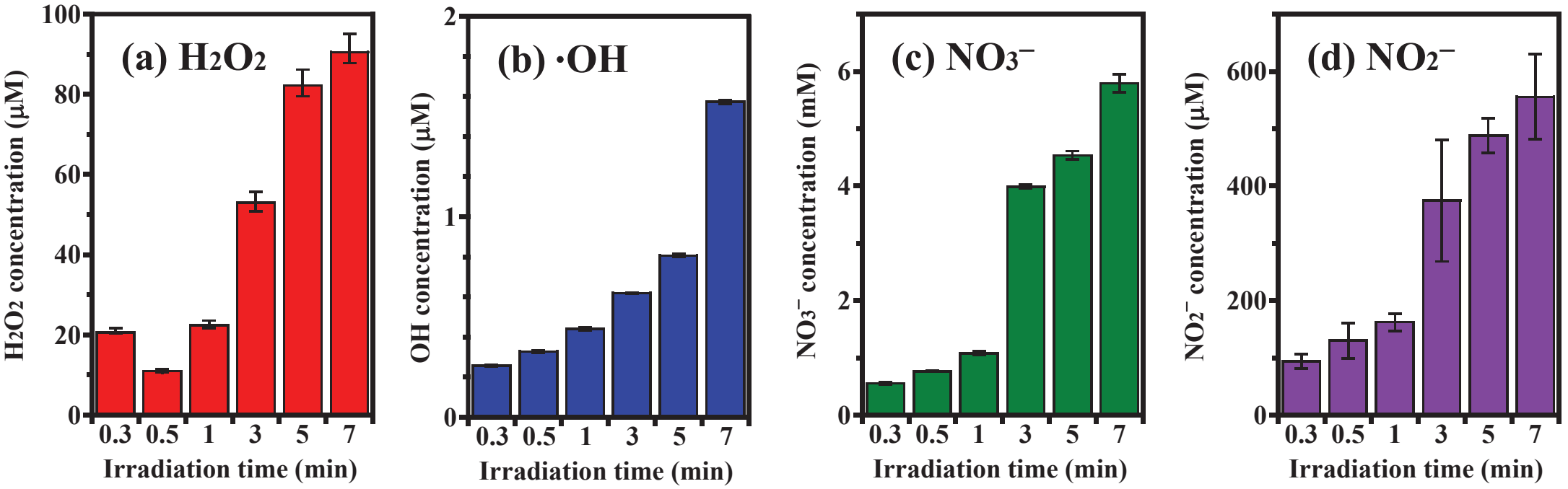

Figure 11. R. Kawakami *et al*.